Reinforcement of silica with single-walled carbon nanotubes through covalent functionalization

Yuanjian Zhang, Yanfei Shen, Dongxue Han, Zhijuan Wang, Jixia Song and Li Niu*

Received 29th August 2006, Accepted 20th September 2006
First published as an Advance Article on the web 5th October 2006
DOI: 10.1039/b612317a

Single-walled carbon nanotubes (SWCNTs) as reinforcing components were extended into silica monoliths and thin films *via* covalent functionalization for the first time. Silica materials have poor mechanical attributes, which limit their applications. Because of the extreme flexibility of SWCNTs and their large interfacial area, they may be very intriguing as reinforcing fillers for the silica matrix. To get more uniform dispersion and stronger interfacial interaction, SWCNTs were covalently functionalized with silane, and then integrated into silica *via* a sol–gel process, and their properties were also compared with those of pristine SWCNTs. Results show that the silane-functionalized nanotubes resulted in better mechanical properties (for example, 33% increase in stress, and 53% increase in toughness), as well as higher electron-transfer kinetics.

1. Introduction

The sol–gel process has played a prominent role in the preparation of various materials with well-tuned structures on the nanometer scale,[1–3] including aerogels, films, fibers, monoliths and powders. By incorporating selected functional molecules carefully, they have found numerous applications in various fields.[2–6] Silica materials are one of the most important and extensively studied,[1,3] but they exhibit poor mechanical attributes such as brittleness and low resistance to mechanical stress, which limit their applications, especially as thin films and bulk monoliths.[3–5,7] So far, on the basis of understanding of the sol–gel process,[1] some synthetic methods, such as critical point extraction,[8] freeze-drying,[3] *etc*., have greatly solved the problem, but the reaction conditions are too demanding. In some cases, mild conditions are highly desired, such as in bioencapsulation and sensors.[4,5] One possible alternative way to bypass the above limitation is to directly reinforce these silica materials with inert fillers such as graphite powder,[9] methylated silica,[10] polymers,[7,11] and so forth.[4,6]

As one kind of truly molecular entity, carbon nanotubes (CNTs) are of significant interest due to their unique electronic, thermal, and mechanical properties, and potential applications.[12–14] Recently, the development of CNTs as reinforcing fillers to overcome the performance limitations of conventional materials has become an interesting concept.[15,16] Most of the attention has been focused on CNT-reinforced polymers,[17–22] ceramics,[23–26] and metals.[27,28] Derived from the extreme flexibility and the large interfacial area of CNTs, it may be very intriguing to consider CNTs as a reinforcing filler for the silica matrix. Moreover, by incorporating these two individual advanced materials, silica and CNTs, many novel applications are expected. For instance, because theory calculation and experiments show CNTs have unique linear and nonlinear optical properties,[29,30] and silica monoliths are often used in optical devices (transmission from UV to near infrared region), CNT-silica monoliths may find applications in the field of optics, such as planar optical wave guides, optical switches and optical limiting devices.[31] Besides, as a coating material, CNT-silica composite would be attractive for electromagnetic interference (EMI) shielding.[32] As yet, however, there are still few investigations focused on CNT-reinforced silica, especially as thin films or bulk monoliths.[33]

In this report, single-walled carbon nanotubes (SWCNTs) were explored as a reinforcing component of silica thin films and bulk monoliths. In order to efficiently reinforce the silica matrix with SWCNTs, two important processing issues had to be addressed: one was the homogeneous dispersion of SWCNTs in the matrix, the other was the strong interfacial interactions required between the SWCNTs and the matrix. The former would ensure that the load was distributed over the total nanotubes, and the latter would ensure that SWCNTs actually carried the load.

However, there are no general solutions to disperse SWCNTs. Their insolubility in solvents due to strong inter-tube van der Waals attraction impedes their applications.[14] Moreover, due to poor interactions between pristine SWCNTs and the silica matrix, pristine SWCNTs very easily agglomerated in the silica matrix, which would greatly inhibit the effective load transfer. Noncovalent or covalent functionalization has been demonstrated to improve solubility.[12–14] Our strategy for solving the above challenges involved the covalent functionalization of SWCNTs with silane and subsequently covalent incorporation of the functionalized SWCNTs into the silica matrix *via* the sol–gel process. Pristine SWCNTs were also utilized for comparison. It was found that the covalent route provided a more homogeneous dispersion of SWCNTs, as well as stronger interfacial linkages between SWCNTs and the matrix, which resulted in both enhanced mechanical properties and electron-transfer kinetics.

State Key Laboratory of Electroanalytical Chemistry, Changchun Institute of Applied Chemistry, and Graduate School of the Chinese Academy of Sciences, Chinese Academy of Sciences, Changchun 130022, P. R. China. E-mail: lniu@ciac.jl.cn; Fax: +86-431-5262800

2. Experimental

2.1 Materials

Pristine SWCNTs (u-SWCNTs, carbon nanotube volume content of $\geqslant$90%, single-walled volume content $\geqslant$50%, length 5–15 μm, diameter <2 nm) were produced by the CVD process and were obtained from Shenzhen Nanotech Port Co. Ltd., China, in purified form. Unless otherwise stated, other reagents were of analytical grade and were used as received.

2.2 Instruments

Fourier transform infrared spectroscopy (FTIR) was carried out on a Bruker Vertex 70 spectrometer (4 cm^{-1}). Raman spectra were measured with a Renishaw 2000 Raman spectrometer (514.5 nm). Low-angle X-ray diffraction (XRD) analyses were recorded on a D/Max 2500 V X-ray diffractometer using Cu-Kα (1.5406 Å) radiation. Scanning electron microscopy (SEM) pictures were imaged by an XL30 ESEM FEG field emission scanning electron microscope. Compressive tests were performed using an Instron 1121 with a crosshead speed of 0.1 mm min^{-1}. X-Ray photoelectron spectroscopy (XPS) was conducted with a VG ESCALAB MK II spectrometer (VG Scientific, UK) employing a monochromatic Mg-Kα X-ray source ($h\gamma$ = 1253.6 eV) and the elemental content ratio was evaluated by using the software installed with the instrument. Electrochemical impedance measurements (EIS) were performed on a CHI 660A electrochemical workstation and were carried out in a conventional three-electrode electrochemical cell with a silica thin film-modified electrode as the working electrode. The auxiliary electrode was a Pt wire and the reference electrode was Ag|AgCl (saturated KCl).

2.3 Functionalization of SWCNTs

Firstly pristine SWCNTs (u-SWCNTs) were modified with carboxylic groups (SWCNTs-COOH) *via* acid treatment[34,35] and then reacted with (3-glycidoxypropyl)trimethoxysilane (GPTMS), as illustrated in Scheme 1. Briefly, SWCNTs-COOH (10 mg) and KOH (1 mg, as cat.) were dispersed in GPTMS (10 mL), and the resulting mixture was stirred and heated to 70 °C for 24 h.[17,36] After that, the GPTMS-functionalized nanotubes (f-SWCNTs) were filtered with a nylon membrane (0.22 μm pores), thoroughly washed with absolute ethanol, and dried under vacuum.

2.4 Preparation of silica thin film modified electrodes for electrochemical impedance measurements

Tetraethoxysilane (TEOS) sol was prepared by hydrolysis of TEOS (5.58 mL) with ethanol (6.42 mL), water (0.6 mL) and hydrochloric acid (10 μL, 0.1 M). GPTMS sol mixed with f-SWCNTs was prepared by hydrolysis of a mixture of GPTMS and f-SWCNTs (200 μL, 1 mg mL^{-1}) with ethanol (260 μL), water (65 μL) and formic acid (5 μL, 88.0%). Then a hybrid sol consisting of TEOS, GPTMS and f-SWCNTs was prepared by mixing the above two sols at the same molar ratio. The silica thin film modified electrode was prepared by casting the hybrid sol (0.5 μL) on a glassy carbon electrode (GCE, d = 3 mm) and was dried in air. The two other silica film modified GCEs without f-SWCNTs and with u-SWCNTs were prepared in a similar way.

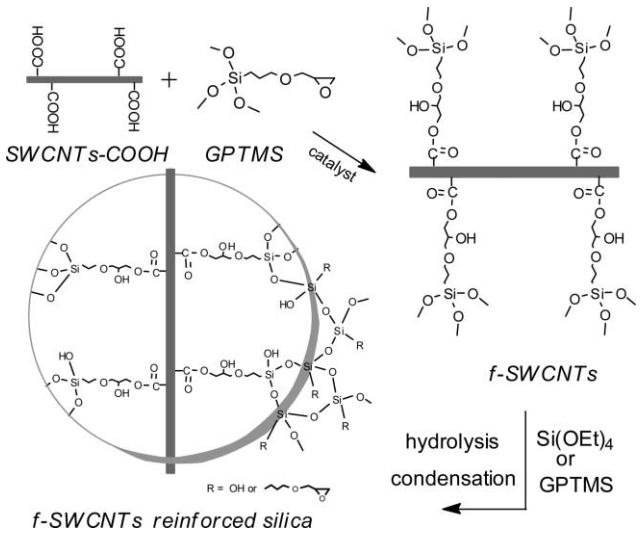

Scheme 1 Illustration of the reaction between SWCNTs-COOH and (3-glycidoxypropyl)trimethoxysilane (GPTMS), and the incorporation of functionalized SWCNTs (f-SWCNTs) into a silica matrix.

2.5 Preparation of silica bulk monoliths for mechanical analysis

A GPTMS sol containing f-SWCNTs was prepared by hydrolysis of f-SWCNTs in GPTMS (250 μL, 1 mg mL^{-1}) with ethanol (60 μL), water (80 μL) and formic acid (5 μL, 88.0%). The neat GPTMS sol and GPTMS sol containing u-SWCNTs were prepared similarly except that no f-SWCNTs or u-SWCNTs were added. Then these three sols were added into cylindrical molds (H = 3 mm and D = 5 mm) and treated at 70 °C for 5 days. In order to avoid dispersing u-SWCNTs in silica monoliths badly, intermittent ultrasonication was utilized. The other two samples were also treated in the same way for consistency.

3. Results and discussion

3.1 Covalent functionalization of SWCNTs with silane

The covalent functionalization of SWCNTs with (3-glycidoxypropyl)trimethoxysilane (GPTMS) was firstly investigated by Fourier transform infrared spectroscopy (FTIR). The characteristic band of the carboxylic group in SWCNTs-COOH appeared at *ca*. 1728 cm^{-1} (C=O) (Fig. 1a top).[34,35] When functionalized with GPTMS, the vibration of C=O shifted to *ca.* 1734 cm^{-1} and the vibration of C–O of the ester appeared at *ca*. 1260 cm^{-1} (Fig. 1a bottom), which confirmed the esterification reaction.[17,36] Moreover, the appearance of bands at *ca*. 3300 (O–H) and 1092 (Si–O–C/C–O–C) cm^{-1} provided more evidence for this successful chemical functionalization.[37] Raman spectra were also used to confirm such a covalent functionalization (Fig. 1b). The bands of sp^3 carbon and sp^2 carbon of SWCNTs appeared at *ca*. 1345 (D band) and 1580 cm^{-1} (G band), respectively.[14,38] Because the D band is diagnostic of disruptions in the hexagonal framework of the

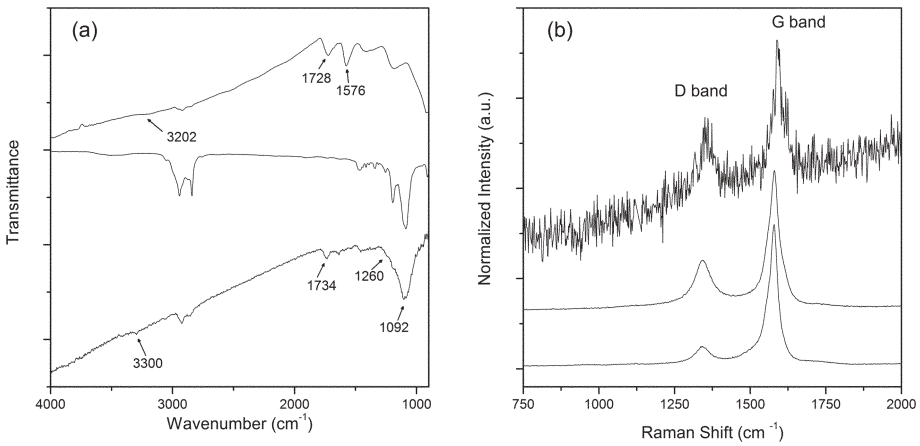

Fig. 1 (a) FTIR spectra of SWCNTs-COOH (top), (3-glycidoxypropyl)trimethoxysilane (GPTMS) (middle) and f-SWCNTs (bottom). (b) Raman spectra of pristine SWCNTs (bottom), SWCNTs-COOH (middle), and f-SWCNTs (top). The intensities were normalized to the G band.

SWCNTs, the relative intensity of this mode will increase if the carbon atoms change from sp^2 to sp^3, *i.e.* covalent functionalization occurs.[14,38] It was observed that from pristine unfunctionalized SWCNTs (u-SWCNTs) to SWCNTs-COOH, and to f-SWCNTs, the relative intensity of the D band increased stepwise, which was in agreement with expectation. The quantified efficiency could be obtained from X-ray photoelectron spectra (XPS). The molar ratio of carbon atoms of SWCNTs to silicon in f-SWCNTs was estimated to be *ca.* 10 : 1. It was rather efficient and comparable to that reported previously.[17,36] Therefore, it is undoubted that GPTMS had been successfully covalently grafted onto SWCNTs.

The morphology of the f-SWCNTs was investigated by scanning electron microscopy (SEM). The mat-like morphology of the f-SWCNTs was observed (Fig. 2). This indicated that these f-SWCNTs remained as bundles or ropes.[20] This was due to the intermolecular hydrogen bonding or possible partial cross-linking by self-condensation of silane between nanotubes. This kind of inter-connection might make single nanotubes link each other so as to prevent the sliding of nanotubes within bundles.[20] Once the functional groups were attached to the nanotubes, the electrostatic repulsion between the nanotubes would overcome the van der Waals interaction to form a stable suspension in the solvent. As shown in Fig. 3, the above covalent functionalization resulted in a more homogenous dispersion of f-SWCNTs in GPTMS and the subsequent sol after brief ultrasonication than that of u-SWCNTs. The most important feature of this covalent functionalization process was that the f-SWCNTs and the sol–gel precursor would be mixed together at much smaller scale.

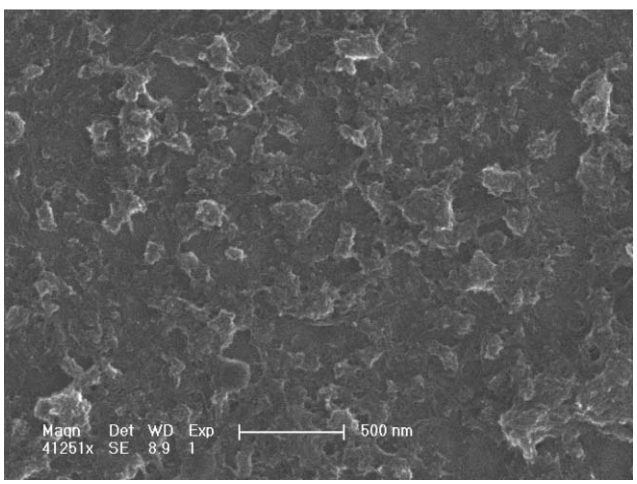

Fig. 2 SEM image of GPTMS functionalized nanotubes (f-SWCNTs).

3.2 Electron-transfer kinetics study

Due to their unique electronic properties, SWCNTs could promote electron-transfer kinetics.[35,39] If the SWCNTs were dispersed more uniformly in the final silica monoliths or thin films, they would offer more electron-transfer pathways so as to decrease the impedance further.[22,40] Therefore, the electrical conductivity of the f-SWCNT-reinforced silica thin film was further investigated by using electrochemical impedance spectroscopy (EIS). It has been reported that the blending of inorganic precursors (*e.g.* TEOS) with organoalkoxysilanes can lead to better electrochemical properties than those prepared alone.[41] Hence, a hybrid sol consisting of TEOS, GPTMS and f-SWCNTs was prepared to examine the effect of dispersion of SWCNTs by the electrical conductivity of the final thin film.

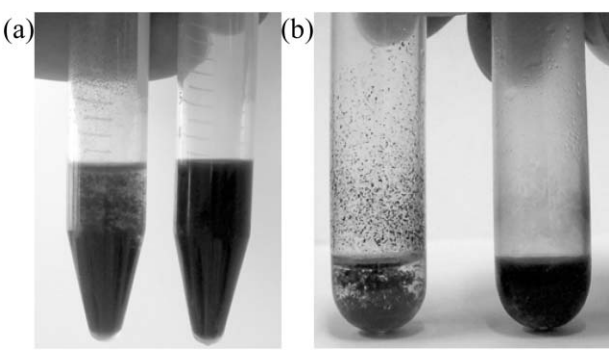

Fig. 3 Photographs of u-SWCNTs (left) and f-SWCNTs (right) dispersed in GPTMS (a) and the subsequent sol (b) after brief ultrasonication.

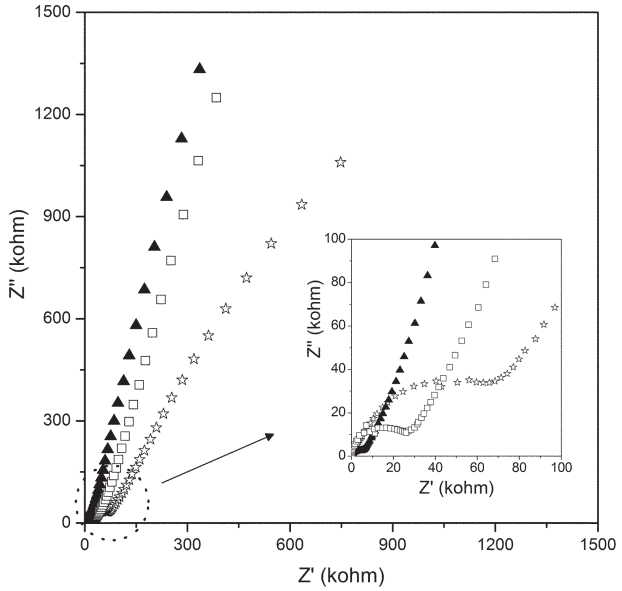

Fig. 4 Nyquist plots of 5 mM $K_4[Fe(CN)_6]$ + 5 mM $K_3[Fe(CN)_6]$ in 0.5 M KCl aqueous solution at GCEs modified with neat TEOS-GPTMS thin film (stars), u-SWCNT-reinforced TEOS-GPTMS thin film (squares), and f-SWCNT-reinforced TEOS-GPTMS thin film (triangles). A sinusoidal potential modulation of ± 5 mV amplitude was superimposed on the open circuit potential. The applied frequency was from 10^5 to 0.1 Hz. Inset: the dotted area in high magnification.

Fig. 4 shows Nyquist plots at different hybrid silica thin film modified glassy carbon electrodes (GCEs). The high-frequency region contains information regarding the kinetics of the faradaic process, and the low-frequency region contains information about the diffusion of the species to the electrode surface. It has been reported that a larger semicircle in the high-frequency region represents slower electron-transfer kinetics and more blocking behavior for the redox couple.[42,43] Here, a very large semicircle was observed at the neat silica thin film modified GCE (Fig. 4, stars). In contrast, the semicircle became smaller at the GCE with u-SWCNT-reinforced silica thin film (squares), and became the smallest at the GCE with f-SWCNT-reinforced silica thin film (triangles). This indicated that the fastest electron-transfer kinetics was achieved by f-SWCNTs with respect to the reference samples. It was also observed that the filling of u-SWCNTs promoted the electron-transfer kinetics, but compared with that of f-SWCNTs it was much smaller. This showed that f-SWCNTs provided more electron-transfer pathways. Therefore, EIS result validated that f-SWCNTs were more homogeneously dispersed in the final thin film than u-SWCNTs.

3.3 Mechanical analysis

The mechanical properties of the reinforced silica monoliths were examined by using compressive tests. For this purpose, a mixture of GPTMS and f-SWCNTs was used as a precursor to prepare f-SWCNT-reinforced GPTMS monoliths, which were molded into cylindrical disk shapes (Fig. 5a inset, right). In control experiments, the u-SWCNT-reinforced GPTMS monolith and neat GPTMS monolith were prepared in a similar way (Fig. 5a inset, middle and left). It was found that the mechanical properties of reinforced monoliths strongly depended on the extent of the load transfer between the monolith and the filling SWCNTs. Fig. 5a shows a stress–strain curve where the compressive failure strength was much increased in the f-SWCNT-reinforced monoliths (triangles), with respect to the neat monoliths (stars) and the u-SWCNT-reinforced monoliths (squares). Moreover, the f-SWCNT-reinforced monoliths had much greater toughness (the area under the stress–strain curve), which corresponded to a stronger material. The complete results of the mechanical properties are summarized and illustrated in Fig. 5b. In the case of the filling of f-SWCNTs, it was clear that both the compressive failure strength and the toughness were greatly improved and much better than those of u-SWCNTs.

To get more information about the interfacial interaction between the monoliths and SWCNTs, fractured sections of the monoliths after compressive tests were further investigated by SEM. As shown in Fig. 6a, most f-SWCNTs were embedded in the silica monolith matrix, and no obvious f-SWCNTs were observed to be pulled out. This indicated that f-SWCNTs had stronger covalent interfacial bonding with the matrix so that the fracture did not occur preferentially at the f-SWCNTs/monolith interface. In contrast, some u-SWCNTs were clearly observed to be pulled out from the silica monolith matrix (Fig. 6b).

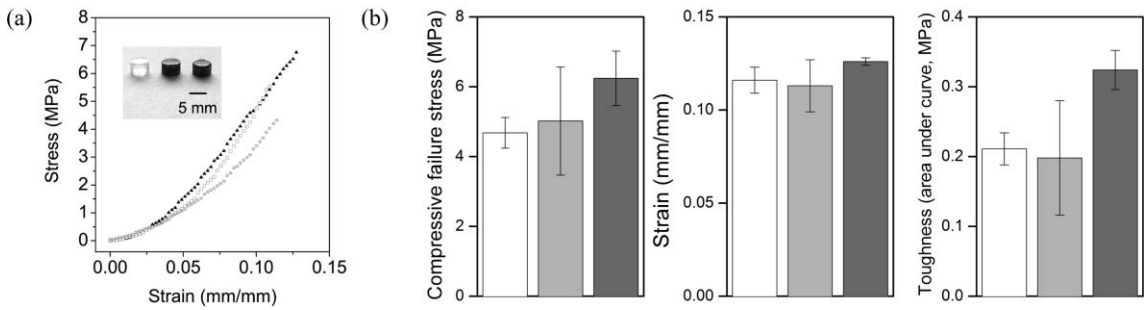

Fig. 5 (a) Stress–strain plots of neat GPTMS monolith (stars), u-SWCNTs-reinforced GPTMS monolith (squares) and f-SWCNTs-reinforced GPTMS monolith (triangles). Inset: photographs of monolith disks for the compressive tests. From left to right: neat GPTMS monolith, u-SWCNT-reinforced GPTMS monolith, and f-SWCNT-reinforced GPTMS monolith. (b) Summarized mechanical properties of monoliths. White column: neat GPTMS monoliths; light gray column: u-SWCNT-reinforced GPTMS monoliths; and dark gray column: f-SWCNTs-reinforced GPTMS monoliths.

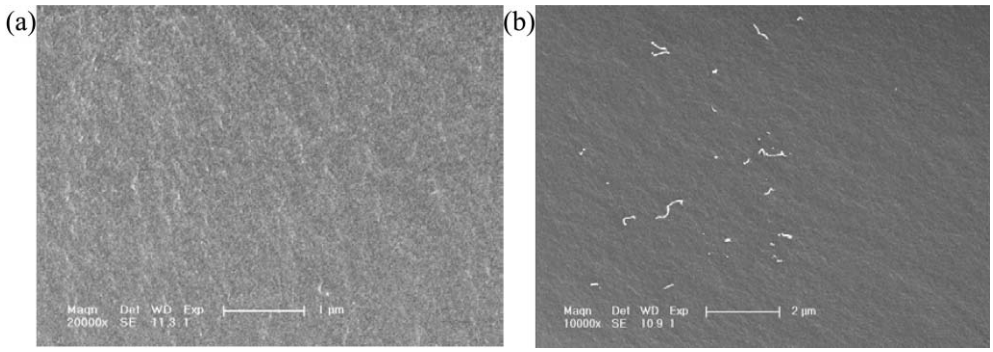

Fig. 6 SEM images of fractured sections of (a) f-SWCNT-reinforced GPTMS monoliths and (b) u-SWCNT-reinforced GPTMS monoliths after the compressive tests.

Hence, due to the uniform dispersion of f-SWCNTs (Fig. 4) and the strong interfacial linkage between the f-SWCNTs and silica monolith matrix (Fig. 6), high load-transfer efficiency of f-SWCNTs in the silica monolith matrix was obtained so as to greatly improve the mechanical properties of silica monoliths (Fig. 5). It should be noted that because SWCNTs have the ability to deform prior to breaking, such uniform dispersion and strong interfacial bonding would lead to high reinforcement both in strength and in toughness,[16] as illustrated in Fig. 5b. In general, high strength and high toughness are difficult to achieve at the same time for common materials. But SWCNT-reinforced composites with strong interfacial linkages do have this unique property.[16] Here the improved strength and toughness were in favor of preventing the cracking of the silica monoliths or thin films.

3.4 Microstructural influence on the silica monolith

While concentrating on the mechanical reinforcement, preserving the original structure of silica is also essential and could not be neglected. Moreover, it was reported that processing-induced structural changes in the matrix might have greater effects on mechanical properties than the actual presence of SWCNTs.[15] Therefore, the microstructures of GPTMS monoliths with and without reinforcement were further examined by using low-angle XRD (Fig. 7). Similar to that of the neat silica monoliths (a), the XRD pattern of the silica monoliths reinforced with f-SWCNTs (c) and with u-SWCNTs (b) both had a broad diffraction peak below 10°. Calculated from the center of the diffraction peaks, the pore size of silica monoliths was only shifted slightly from 1.4 nm to 1.5 nm after the reinforcements. This indicated that the process of reinforcement itself did not cause significant changes of the distorted 3D micro-structure of silica monoliths. The remarkable improvement of the mechanical properties of the silica monoliths here originated from the high load-transfer efficiency of f-SWCNTs in the silica monolith matrix.

Therefore, f-SWCNTs displayed more distinct reinforcement of silica in comparison with u-SWCNTs; meanwhile the original micro-structure of the silica was retained. The covalent functionalization of SWCNTs with the silane played an important role. On one hand, due to the like-to-like principle, silane covalently anchored on SWCNTs would help the SWCNTs to disperse more uniformly in the precursor, and in the final monolith or thin film. Better homogeneous dispersion would make more nanotube surfaces available for interacting with the surrounding silica matrix. On the other hand, the silane acted as a covalent "hinge", which would offer stronger interfacial interactions between SWCNTs and the silica matrix. Taking these two merits into account, more effective load transfer to the matrix was obtained. Furthermore, covalent functionalization of SWCNTs with the silane would not introduce other impure molecules and did not require any further separation after the reinforcement. It had been reported that surfactants could also improve the dispersion of SWCNTs in silica sols, but finally they have to be removed for further applications.[44]

In addition, our study indicated clearly that the electron-transfer kinetics of silica thin films was also significantly enhanced by the filling of f-SWCNTs (Fig. 4). Because one of the major challenges in electrochemical applications of silica thin films was to ensure high electron-transfer kinetics through the films,[4] and it had been reported that CNTs-silica composites had potential capabilities for the development of electrochemical devices,[45,46] our results here provided a

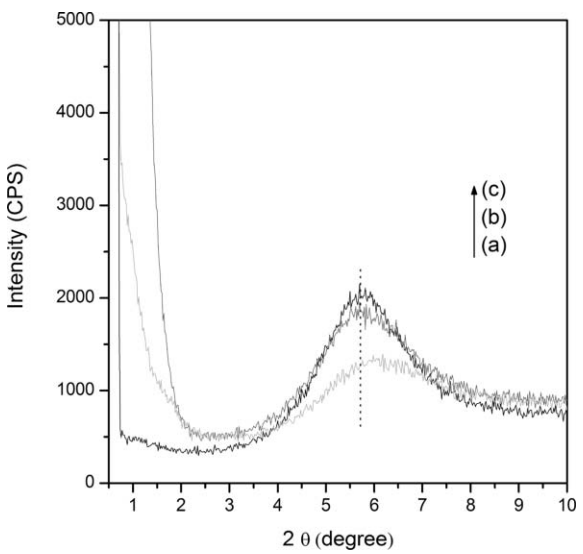

Fig. 7 Low-angle X-ray diffraction (XRD) patterns of neat GPTMS monoliths (a), u-SWCNT-reinforced GPTMS monoliths (b), and f-SWCNT-reinforced GPTMS monoliths (c).

potential improved method. In these previous reports only un-functionalized carbon nanotubes were used; our results here indicate that functionalized carbon nanotubes might have better performance in these electrochemical devices. Besides, by incorporating these two individual advanced materials, silica and SWCNTs, many other novel applications are expected, such as optical devices and electromagnetic interference (EMI) shielding.

4. Conclusion

The application of SWCNTs as a reinforcing component was extended to silica monoliths and thin films *via* covalent functionalization for the first time. Owing to the like-to-like principle, functionalization of SWCNTs with silane improved the homogeneous dispersion of SWCNTs in the silica matrix. Moreover, it also offered covalent bonding between the nanotubes and the silica matrix, which resulted in improved interfacial interactions. Owing to these improvements, the covalent filling of SWCNTs in silica achieved both enhanced strength and toughness. This should facilitate applications of silica monoliths and thin films, which were previously limited by their poor mechanical properties, such as in bioencapsulation and electrochemistry. Furthermore, the electron-transfer kinetics of silica was also significantly enhanced by the covalent filling of SWCNTs, which should promote the application of silica-SWCNT composites in future electronic devices. The ratio of SWCNTs to alkoxysilane was 1 mg mL^{-1} here. A higher ratio of SWCNTs to the matrix might be expected to result in greater reinforcement,[18,20] but larger quantities of SWCNTs in the silica matrix would be unfavorable to homogeneous dispersion. These problems together with other applications of SWCNT-reinforced silica will be further investigated in the near future.

Acknowledgements

The authors are most grateful to the NSFC, China (No. 20475053) and to Department of Science and Technology of Jilin Province (No. 20050102) for financial support.

References

1 L. L. Hench and J. K. West, *Chem. Rev.*, 1990, **90**, 33–72.
2 *Handbook of Sol–Gel Science and Technology: Processing, Characterization and Applications*, ed. S. Sakka, Kluwer, Dordrecht, 2005.
3 N. Hüsing and U. Schubert, *Angew. Chem., Int. Ed.*, 1998, **37**, 22–45.
4 A. Walcarius, *Chem. Mater.*, 2001, **13**, 3351–3372.
5 I. Gill, *Chem. Mater.*, 2001, **13**, 3404–3421.
6 A. Walcarius, D. Mandler, J. A. Cox, M. Collinson and O. Lev, *J. Mater. Chem.*, 2005, **15**, 3663–3689.
7 H. Yang, Q. Shi, B. Tian, S. Xie, F. Zhang, Y. Yan, B. Tu and D. Zhao, *Chem. Mater.*, 2003, **15**, 536–541.
8 C. G. Göltner, S. Henke, M. C. Weissenberger and M. Antonietti, *Angew. Chem., Int. Ed.*, 1998, **37**, 613–616.
9 M. Tsionsky, G. Gun, V. Glezer and O. Lev, *Anal. Chem.*, 1994, **66**, 1747–1753.
10 I. Gill and A. Ballesteros, *J. Am. Chem. Soc.*, 1998, **120**, 8587–8598.
11 B. Q. Wang, B. Li, Z. X. Wang, G. B. Xu, Q. Wang and S. J. Dong, *Anal. Chem.*, 1999, **71**, 1935–1939.
12 P. M. Ajayan, *Chem. Rev.*, 1999, **99**, 1787–1800.
13 A. Bianco and M. Prato, *Adv. Mater.*, 2003, **15**, 1765–1768.
14 Special Issue on Carbon Nanotubes in *Acc. Chem. Res.*, ed. R. C. Haddon, 2002, **35**, pp. 997–1113.
15 W. A. Curtin and B. W. Sheldon, *Mater. Today*, 2004, **7**(11), 44–49.
16 H. D. Wagner and R. A. Vaia, *Mater. Today*, 2004, **7**(11), 38–42.
17 J. Zhu, J. D. Kim, H. Q. Peng, J. L. Margrave, V. N. Khabashesku and E. V. Barrera, *Nano Lett.*, 2003, **3**, 1107–1113.
18 C. Velasco-Santos, A. L. Martinez-Hernandez, F. T. Fisher, R. Ruoff and V. M. Castano, *Chem. Mater.*, 2003, **15**, 4470–4475.
19 M. B. Bryning, M. F. Islam, J. M. Kikkawa and A. G. Yodh, *Adv. Mater.*, 2005, **17**, 1186–1191.
20 J. Zhu, H. Peng, F. Rodriguez-Macias, J. L. Margrave, V. N. Khabashesku, A. M. Imam, K. Lozano and E. V. Barrera, *Adv. Funct. Mater.*, 2004, **14**, 643–648.
21 J. N. Coleman, M. Cadek, R. Blake, V. Nicolosi, K. P. Ryan, C. Belton, A. Fonseca, J. B. Nagy, Y. K. Gun'ko and W. J. Blau, *Adv. Funct. Mater.*, 2004, **14**, 791–798.
22 Y. S. Song and J. R. Youn, *Carbon*, 2005, **43**, 1378–1385.
23 G. D. Zhan, J. D. Kuntz, J. L. Wan and A. K. Mukherjee, *Nat. Mater.*, 2003, **2**, 38–42.
24 L. An, W. Xu, S. Rajagopalan, C. Wang, H. Wang, Y. Fan, L. Zhang, D. Jiang, J. Kapat, L. Chow, B. Guo, J. Liang and R. Vaidyanathan, *Adv. Mater.*, 2004, **16**, 2036–2040.
25 A. Peigney, *Nat. Mater.*, 2003, **2**, 15–16.
26 X. T. Wang, N. P. Padture and H. Tanaka, *Nat. Mater.*, 2004, **3**, 539–544.
27 S. I. Cha, K. T. Kim, S. N. Arshad, C. B. Mo and S. H. Hong, *Adv. Mater.*, 2005, **17**, 1377–1381.
28 E. Flahaut, A. Peigney, C. Laurent, C. Marliere, F. Chastel and A. Rousset, *Acta Mater.*, 2000, **48**, 3803–3812.
29 G. Y. Guo, K. C. Chu, D.-s. Wang and C.-g. Duan, *Phys. Rev. B*, 2004, **69**, 205416–205411.
30 H. Kataura, Y. Kumazawa, Y. Maniwa, I. Umezu, S. Suzuki, Y. Ohtsuka and Y. Achiba, *Synth. Met.*, 1999, **103**, 2555–2558.
31 J. E. Riggs, D. B. Walker, D. L. Carroll and Y. P. Sun, *J. Phys. Chem. B*, 2000, **104**, 7071–7076.
32 Y. L. Yang and M. C. Gupta, *Nano Lett.*, 2005, **5**, 2131–2134.
33 H. B. Zhan, C. Zheng, W. Z. Chen and M. Q. Wang, *Chem. Phys. Lett.*, 2005, **411**, 373–377.
34 J. Zhang, H. Zou, Q. Qing, Y. Yang, Q. Li, Z. Liu, X. Guo and Z. Du, *J. Phys. Chem. B*, 2003, **107**, 3712–3718.
35 Y. J. Zhang, J. Li, Y. F. Shen, M. J. Wang and J. H. Li, *J. Phys. Chem. B*, 2004, **108**, 15343–15346.
36 A. Eitan, K. Jiang, D. Dukes, R. Andrews and L. S. Schadler, *Chem. Mater.*, 2003, **15**, 3198–3201.
37 *Handbook of Analytical chemistry: Spectroscopy Analysis*, ed. Y. Ke and H. Dong, Chemical Industry Press, Beijing, China, 1998.
38 Y. Zhang, Y. Shen, J. Li, L. Niu, S. Dong and A. Ivaska, *Langmuir*, 2005, **21**, 4797–4800.
39 E. Katz and I. Willner, *ChemPhysChem*, 2004, **5**, 1084–1104.
40 T. Katakabe, T. Kaneko, W. Watanabe, T. Fukushima and T. Aida, *J. Electrochem. Soc.*, 2005, **152**, A1913–A1916.
41 M. M. Collinson, *TrAC, Trends Anal. Chem.*, 2002, **21**, 30–38.
42 T. H. Silva, V. Garcia-Morales, C. Moura, J. A. Manzanares and F. Silva, *Langmuir*, 2005, **21**, 7461–7467.
43 H. Gu, X. d. Su and K. P. Loh, *J. Phys. Chem. B*, 2005, **109**, 13611–13618.
44 J. W. Ning, J. J. Zhang, Y. B. Pan and J. K. Guo, *Ceram. Int.*, 2004, **30**, 63–67.
45 V. G. Gavalas, R. Andrews, D. Bhattacharyya and L. G. Bachas, *Nano Lett.*, 2001, **1**, 719–721.
46 K. P. Gong, M. N. Zhang, Y. M. Yan, L. Su, L. Q. Mao, Z. X. Xiong and Y. Chen, *Anal. Chem.*, 2004, **76**, 6500–6505.